Upregulation of Bag3 Exacerbates Cervical Cancer Progression by Impairing Immune Response and Inhibiting Cell Ferroptosis

Yan Zhang
Wuhan University Renmin Hospital https://orcid.org/0000-0001-7798-531X
Jun Zhang
Renmin Hospital of Wuhan University
Yanping Jiang
Renmin Hospital of Wuhan University
Yuzi Zhao
Renmin Hospital of Wuhan University
Aili Tan
Renmin Hospital of Wuhan University
Lu Wang
Renmin Hospital of Wuhan University
Shujun Wang
Renmin Hospital of Wuhan Hospital
Jie Pi
Renmin Hospital of Wuhan Hospital
Lin Mao
Renmin Hospital of Wuhan Hospital
Xing Li (xin_yue_0817@163.com)
https://orcid.org/0000-0002-5179-1426

Primary research

Keywords: cervical cancer, Bag3, immune response, ferroptosis

Posted Date: August 14th, 2020

DOI: https://doi.org/10.21203/rs.3.rs-57265/v1

Abstract

Background: Cervical cancer remains a serious threat to women worldwide. Thus, effective strategies to treat cervical cancer are urgently needed. Bcl-2-associated athanogene 3 (Bag3) has been shown to be increased in several malignant neoplasms. However, little is known about the function of Bag3 in cervical cancer. We aimed to evaluate the function of Bag3 in cervical cancer progression.

Method: qRT-PCR was carried out to test mRNA expression of Bag3, SLC7A11 and SLC3A2. Western blot analysis was conducted to detect protein expression of Bag3, SLC7A11 and SLC3A2. Cell proliferation was assessed using CCK-8, EdU and Colony formation assay. Flow cytometry assay was used to determine the frequency of IFN-γ- or TNF-α-producing $CD8^+$ T cells. Transwell migration and invasion assay were carried out to detect cell migration and invasion capacity. Immunohistochemical staining was carried out to assess Bag3 and CD3 expression

Results: Bag3 was obviously elevated in cervical cancer tissues than in the adjacent normal tissues. Bag3 mRNA was upregulated in different cervical cancer cells (SiHa, C-33A, HT-3, and HeLa cells). SiHa cell proliferation, colony formation, and migration/invasion capacity were enhanced by Bag3 overexpression. Bag3 inhibited the immune response in cervical cancer. After C57BL6 mice were injected with Bag3-overexpressing SiHa cells, infiltrating $CD3^+$ T cells around tumors were reduced. IFN-γ- and TNF-α-producing $CD8^+$ T cells in tumor sections were remarkably inhibited by Bag3. Moreover, Ki-67^+- and CD107a-producing $CD8^+$ T cells were also suppressed. Bag3 repressed SiHa cell ferroptosis. Bag3 deletion inhibited cervical cancer development by improving the immune response and inducing ferroptosis.

Conclusions: Taken together, these results indicated that Bag3 contributes to cervical cancer progression by impairing immune response and repressing cell ferroptosis.

Background

Cervical cancer is the most frequent gynecological malignant tumor in women worldwide. An increasing number of cervical cancer incidences and mortalities each year has been reported in many countries, especially developing countries [1-3]. The main treatment strategies for cervical cancer include radical surgery, radiotherapy, and chemotherapy. However, for cervical cancer patients in the advanced stages, these strategies exhibit limited treatment efficacy [4]. Hence, it is important to study the mechanism of cervical cancer and identify effective gene targets for its treatment.

Bag3 is a member of the human BAG co-chaperone family [5]. BAG3 plays various roles in cellular processes [6,7]. BAG3 expression is significantly increased in some neoplastic tissues. For example, in breast cancer, Bag3 can induce the stem cell-like phenotype by upregulating CXCR4 [8]. Deletion of Bag3 represses cisplatin resistance in ovarian cancer cells by inhibiting autophagy [9]. Bag3 is closely associated with colorectal cancer progression and chemoresistance [10]. Additionally, it has been shown

that loss of Bag3 greatly represses the EMT process in human cervical cancer cells [11]. Down-modulation of Bag3 can sensitize HeLa cells to PEITC-triggered apoptosis and rescue p53 [12].

Currently, Bag3 is remarkably upregulated in cervical cancer. Upregulation of Bag3 promotes the progression of cervical cancer, while knockdown of Bag3 represses cervical cancer development. Additionally, up-regulation of Bag3 inactivates immune responses and ferroptosis, whereas Bag3 deletion demonstrated an opposite phenomenon. Therefore, we hypothesized that Bag3 contributes to cervical cancer progression involving the immune response and cell ferroptosis.

Materials And Methods

Clinical tissue specimens

Thirty pairs of cervical cancer tissues and matched adjacent normal tissues were collected from female patients undergoing surgery in Renmin Hospital of Wuhan University between April 2015 and August 2017. We obtained all tissues using microdissection. Tissues were frozen in liquid nitrogen and stored at -80°C. Our current study was approved by the Medical Ethics Committee of Renmin Hospital of Wuhan University. All patients provided written informed consent before the study.

Cell culture

SiHa, C-33A, HT-3, and HeLa cells were obtained from the Cell Bank of the Chinese Academy of Sciences (Shanghai, China). Human cervical surface epithelial cell line, HcerEpic, was purchased from ATCC (Manassas, VA, USA). Cells were incubated in DMEM supplemented with 10% FBS, 100 U/mL penicillin, and 100 μg/mL streptomycin. Cells were grown in a humidified incubator with 5% CO2 at 37°C.

Lentiviral vector infection

A forced Bag3 overexpression assay was carried out by lentiviral transfection in SiHa cells. Briefly, the lentivirus Bag3 and Bag3 shRNA sequences were purchased from Sunbio (Sunbio Medical Biotechnology, Guangzhou, China). SiHa cells were transduced with Lenti-Bag3 or Lenti-NC, along with 12 μg/ml polybrene (Gibco, USA) at an MOI of 15-25. Selection was carried out by treating transduced cells with 1 mg/mL blasticidin for 5 days.

CCK8 assay

Cell proliferation was assessed using a CCK-8 assay kit (Dojindo, Japan). Cells were seeded separately in 96-well plates overnight. After transfection, 10 μL CCK8 solution was added for 1 h and absorbance readings at 450 nm were recorded using a microplate reader (Bio-Tek, Winooski, VT, USA).

EdU assay

EdU incorporation assay was carried out using a Cell-LightTM EdU Apollo®567 In Vitro Imaging kit (RiboBio, Guangzhou, China). Cells were plated into 96-well plates (2000 cells per well) for a whole night.

The cells were then treated with 50 μM EdU for 2 h. Cells were fixed using 4% formaldehyde solution and stained using Apollo and Hoechst 33342. A fluorescence microscope (Olympus Corporation, Tokyo, Japan) was used.

Colony formation

Cells were fixed using 10% formaldehyde and stained with 0.1% crystal violet for a minute. Then, we discarded the staining solution and washed each well. Subsequently, the cells were visualized under a fluorescence microscope (AF6000, Leica Microsystems GmbH, Wetzlar, Germany).

Transwell migration and invasion assays

After cells were collected using trypsinization/EDTA, they were placed into transwell chambers (Corning, USA) to carry out the migration assay. For the invasion assay, 1×10^4 cells were placed into the upper chambers coated with 150 mg Matrigel. After incubation at 37 °C, the cells remaining on the upper surface were removed. Then, crystal violet was used to stain the cells on the lower surface. We visualized the stained cells and counted them using a light microscope.

qRT-PCR

Total RNA was isolated using TRIzol® reagent (Life Technology, Thermo Fisher Scientific, Waltham, MA, USA). Then, cDNAs were synthesized using M-MLV Reverse Transcriptase (Promega, Madison, WI, USA). Subsequently, qRT-PCR was conducted using the SYBR®Premix Ex Taq™ II kit (Takara, Otsu, Japan). Primers are listed in **Table 1**. Relative expression was quantified using the $2^{-\Delta\Delta Ct}$ method.

Immunoblotting analysis

After cells were washed with ice-cold PBS, they were treated with RIPA lysis buffer. We quantified protein concentrations using a BCA protein assay kit (Beyotime, Haimen, China). Proteins were separated on 10% SDS-PAGE gels and transferred onto PVDF membranes. Membranes were incubated with anti-Bag3, anti-SLC7A11, anti-SLC3A2, and anti-β-actin (1:1000 dilution; Abcam, USA) antibodies. Then, HRP-conjugated secondary antibodies were used. Afterward, blots were observed using an ECL detection system.

Lipid ROS assay

Lipid ROS levels were tested using 5 μM of BODIPY-C11 dye. Cells were plated in six-well plates. Culture medium was replaced with 2 ml of medium with 5 μM of BODIPY-C11. Cells were collected in 15 ml tubes. The cell suspension was filtered through a cell strainer and flow cytometry analysis was carried out to detect the amount of ROS. Subsequently, the fluorescence intensities of cells were examined using a BD FACSAria cytometer (BD Biosciences, San Jose, California, USA).

Immunohistochemical analysis

Tumor specimens were derived from routine formalin-fixed, paraffin-embedded tissue samples. Sections (3-μm thick) were cut from the paraffin blocks and mounted on silanized slides. Staining for Bag3 and CD3 was carried out using the Bag3 and CD3 antibodies (1:200 dilution; Abcam, Cambridge, UK) for a whole night at 4°C. For all slides, the immune reaction was induced with DAB.

Flow cytometry

Cells were stained with anti-CD8-APC, anti-IFNγ-PE, or anti-TNF-α-FITC. We analyzed the stained cells on an LSRII® flow cytometer (BD Biosciences, San Jose, California, USA). Data were analyzed using FlowJo software (Tree Star, Ashland, OR, USA).

Orthotopic xenograft study

To establish an orthotopic mouse model of cervical cancer, six-week-old female athymic nude mice were purchased from Shanghai Animal Laboratory Center. Mice were maintained in a pathogen-free environment. Procedures were conducted according to the protocol approved by the UTHSC Institutional Animal Care and Use Committee. SiHa cells (4×10^6) infected with Bag3 OE or Bag3 shRNA were dispersed in 100 μL PBS and 100 μL Matrigel. Cells were injected directly into the cervix without surgery. We monitored the mice periodically to observe tumor development. A digital Vernier caliper was used to test the tumor volume from one week after injection using the formula: volume (mm^3) = length × width × width/2 . Mice were killed after 17 days post-injection.

Statistical analysis

Statistical analysis was performed using GraphPad Prism 6 software (GraphPad Software, Inc., La Jolla, USA). Statistically significant groups were determined using Student's t-test or one-way analysis of variance (p-value less than 0.05 indicates statistical significance).

Table 1. Primers for real-time PCR

Genes	Forward (5'-3')	Reverse (5'-3')
GAPDH	AAGAAGGTGGTGAAGCAGGC	GTCAAAGGTGGAGGAGTGGG
Bag3	CATTGATGTCCCAGGTCAAG	ATCGGTTCCGAGTCTGATTT
SLC7A11	CATCGTCCTTTCAAGGTGC	ATAGAGGGAAAGGGCAACC
SLC3A2	ACCCCTGTTTTCAGCTACGG	GGTC TTCACTCTGGCCCTTC

Results

Bag3 is elevated in cervical cancer.

Thirty pairs of adjacent normal tissues and cervical cancer tissues were collected from patients with cervical cancer. As exhibited in **Figure. 1a,** qRT-PCR analysis indicated that Bag3 level was obviously increased in cervical cancer tissues than in the adjacent normal tissues. In addition, IB analysis showed that Bag3 protein in adjacent normal tissues was highly overexpressed in cervical cancer tissues, which was chosen from three random patients (**Figure. 1b)**. Immunohistochemistry of paraffinized samples was conducted and we found strong Bag3 staining in cervical cancer tissues, as shown in **Figure. 1c**. Bag3 mRNA levels in different cervical cancer cells (SiHa, C-33A, HT-3, and HeLa cells) were analyzed; it was significantly increased in these cells (**Figure. 1d**. These results indicate that Bag3 is greatly elevated in cervical cancer.

Bag3 promotes cervical cancer progression.

To investigate the detailed effect of Bag3 in cervical cancer, SiHa cells were infected with Bag3 overexpression lentivirus. Elevated Bag3 protein levels were successfully induced in SiHa cells, as shown in **Figure. 2a.** The CCK8 assay was carried out and we demonstrate that SiHa cell survival was enhanced by Bag3 (**Figure. 2b)**. EdU assay analysis demonstrated that SiHa cell proliferation was induced by overexpression of Bag3, as displayed in **Figure. 2c**. A colony formation assay was performed, and we found that SiHa cell colony formation was induced by Bag3 (**Figure 2d)**. Transwell migration and invasion assays indicated that SiHa cell migration and invasion capacity was promoted by Bag3, as shown in **Figure. 2e and 2f.** These results indicate that overexpression of Bag3 contribute to cervical cancer development.

Bag3 restrains the immune response in cervical cancer.

C57BL6 mice were orthotopically injected with control and Bag3-overexpressed SiHa cells to confirm the effect of Bag3 on cervical cancer in vivo. Tumor volume increased in a time-dependent manner as shown in **Figure. 3a**. Additionally, the survival was significantly decreased by the overexpression of Bag3, as shown in **Figure. 3b.** Infiltrating $CD3^+$ T cells around tumors were quantified; these cells were greatly reduced in the Bag3 overexpression group (**Figure. 3c)**. Additionally, the frequency of IFN-γ- and TNF-α-producing $CD8^+$ T cells in tumor sections was evaluated using flow cytometry. IFN-γ- and TNF-α-producing $CD8^+$ T cells were remarkably inhibited by Bag3 upregulation (**Figure. 3d)**. Then, the frequency of Ki-67^+- and CD107a-producing $CD8^+$ T cells in tumor sections was quantified. Ki-67^+- and CD107a-producing $CD8^+$ T cells were restrained, as shown in **Figure. 3e.** In **Figure. 3f,** immunohistochemical analysis of Ki-67 level was highly stained in Bag3-overexpressed tumors. These results indicate that Bag3 greatly represses immune response in cervical cancer.

Bag3 inhibits ferroptosis of SiHa cells

Flow cytometry analysis indicated that lipid ROS was reduced by Bag3 overexpression in SiHa cells (**Figure. 4a**). SLC3A2 and SLC7A11 are two subunits of the glutamate-cystine antiporter system xc-, which can promote tumor cell lipid peroxidation and ferroptosis. As shown in **Figure. 4b and 4c,** SLC7A11, and

SLC3A2 expression was repressed by Bag3, which was rescued by the ferroptosis inducer Erastin. The induced colony formation ability of SiHa cells was inhibited by 1μM Erastin, as shown in **Figure. 4d**. Additionally, the induced migration and invasion ability of SiHa cells facilitated by Bag3 overexpression was significantly reduced by Erastin treatment (**Figure 4c and 4f**) These results indicate that Bag3 greatly inhibits the ferroptosis in SiHa cells.

Loss of Bag3 ameliorates the development of cervical cancer.

Bag3 was repressed by Bag3 shRNA resulting in greatly reduced levels of Bag3 protein in SiHa cells (**Figure. 5a**). In **Figure. 5b,** we show that ROS levels were induced by Bag3 shRNA in SiHa cells. SLC7A11 and SLC3A2 mRNA levels were analyzed by qRT-PCR; their levels were significantly increased by the loss of Bag3 (**Figure. 5c**). EdU assay analysis demonstrated that SiHa cell proliferation was suppressed by Bag3 deletion (**Figure. 5d**. Bag3-shRNA was infected into SiHa cells and the cells were injected orthotopically into mice. Tumor volume and survival were reduced by downregulation of Bag3, as indicated in **Figure. 5e and 5f**. Immunohistochemical analysis using anti-CD3 antibodies revealed that infiltrating $CD3^+$ T cells around tumors were increased (**Figure. 5g**). Moreover, IFN-γ- and TNF-α-producing $CD8^+$ T cells in tumor sections, as evidenced by flow cytometry, were obviously induced by Bag3 deletion (**Figure. 5h and 5i**). These results demonstrate that the loss of Bag3 ameliorates the development of cervical cancer by improving the immune response and triggering ferroptosis.

Discussion

Here, we demonstrated that Bag3 was obviously elevated in cervical cancer tissues. Additionally, Bag3 mRNA expression in various cervical cancer cells (SiHa, C-33A, HT-3, and HeLa cells) were analyzed. We found that significantly increased levels of Bag3 mRNA in cervical cancer cells. Next, Bag3 was overexpressed in SiHa cells by infecting the Bag3 lentivirus. Overexpression of Bag3 remarkably increased cervical cancer progression by inhibiting immune responses and suppressing cell ferroptosis. Conversely, the loss of Bag3 displayed a reversed phenomenon. In summary, we found that Bag3 contributed substantially to cervical cancer progression via impairing the immune response and reducing cell ferroptosis.

Bag3 contains a conserved domain that can bind to the ATPase domain of Hsp70 [13]. It has been reported that Bag3 can mediate protein delivery, regulate apoptosis, and demonstrate a crucial role in cell adhesion and migration [14]. Additionally, Bag3 levels are elevated in various cancers. For instance, in chronic lymphocytic leukemia, overexpression of Bag3 acts as a marker of poor prognosis [15]. Bag3 expression in glioblastoma cells can induce ubiquitinated client accumulation dependent on Hsp70 [16]. A recent study pointed out that Bag3 expression is closely correlated with the grade of dysplasia, which supports the involvement of Bag3 in cervical carcinogenesis [17]. In addition, Bag3 has been reported to be targeted by miR-206 in human cervical cancer progression [18]. In colorectal cancer, miR-217-5p can induce cell apoptosis by targeting BAG3 in vitro [19]. We found that Bag3 was greatly increased in cervical cancer, and its overexpression hastened cervical cancer development.

It is well established that the local immune response is a crucial determinant of cervical tumorigenesis [20]. In our current study, we found that overexpression of Bag3 repressed $CD3^+$ T cells around local tumors. In addition, IFN-γ- and TNF-α-producing $CD8^+$ T cells were also greatly reduced by Bag3 in tumor sections. These results indicate that Bag3 repressed cervical cancer progression by impairing the immune response.

Reprograming of cellular metabolism, such as the modulation of apoptotic and necrotic cell death, is important for tumorigenesis [21,22]. Ferroptosis is a type of cell death dependent on iron and is an oxidative stress-associated cell death, which is modulated by lipid peroxidation [23,24]. Accumulation of iron, glutathione depletion, and lipid membrane oxidation can contribute to ferroptosis [25,26].The number of reported ferroptosis inducers has been increasing in the recent years [27]. Erastin is a cell-permeable piperazinyl-quinazolinone compound that can induce ferroptosis in cancer cells [28-30]. In the current study, we demonstrated that lipid ROS accumulation was reduced by Bag3 overexpression in SiHa cells. Meanwhile, SLC7A11 and SLC3A2 expression were greatly repressed by Bag3, and the ferroptosis inducer Erastin reversed this. Overexpression of Bag3 significantly repressed SiHa cell ferroptosis.

A recent study reported that CD8+ T cells activated by immunotherapy can induce ferroptosis-specific lipid peroxidation in cancer cells, and ferroptosis promotes the anti-tumor efficacy of immunotherapy [31]. Additionally, IFN-gamma derived from CD8+ T cells can enhance tumor lipid oxidation and ferroptosis [32]. In our current work, we observed that loss of Bag3 ameliorated the development of cervical cancer by inducing immune responses and ferroptosis. Bag3 is a crucial molecule in maintains oncogenic features of cancer cells through diverse mechanisms. In our future study, we would like to investigate more other functions of Bag3 in cervical cancer.

Conclusion

In conclusion, we reported that overexpression of Bag3 promoted cervical cancer progression by impairing immune response and suppressing cell ferroptosis.

Declarations

Ethics approval and consent to participate

The study was approved by the Medical Ethics Committee of Renmin Hospital of Wuhan University, and all patients provided written informed consent before the study.

Consent for publication

Not applicable.

Availability of data and materials

The datasets used during the current study are available from the corresponding author on reasonable request.

Competing interests

The authors declare that they have no competing interests.

Funding

Not applicable.

Authors' contributions

Xing Li designed and supervised the study; **Yan Zhang**, **Jun Zhang** and **Yanping Jiang** performed the experiments; **Yuzi Zhao**, **Aili Tan** and **Lu Wang** collected and did the analysis; **Shujun Wang**, **Jie Pi** and **Lin Mao** supported the study; **Yan Zhang** prepared the manuscript; **Xing Li** revised the manuscript; All authors read and approved the final manuscript.

Acknowledgments

Not applicable.

References

1. Siegel RL, Miller KD, Jemal A. Cancer statistics, 2016. CA: a cancer journal for clinicians 2016;66(1):7-30.
2. Chen W, Zheng R, Baade PD et al. Cancer statistics in China, 2015. CA: a cancer journal for clinicians 2016;66(2):115-132.
3. Di J, Rutherford S, Chu C. Review of the Cervical Cancer Burden and Population-Based Cervical Cancer Screening in China. Asian Pacific journal of cancer prevention : APJCP 2015;16(17):7401-7407.
4. Wright JD, Huang Y, Ananth CV et al. Influence of treatment center and hospital volume on survival for locally advanced cervical cancer. Gynecologic oncology 2015;139(3):506-512.
5. Takayama S, Xie Z, Reed JC. An evolutionarily conserved family of Hsp70/Hsc70 molecular chaperone regulators. The Journal of biological chemistry 1999;274(2):781-786.
6. Rosati A, Graziano V, De Laurenzi V, Pascale M, Turco MC. BAG3: a multifaceted protein that regulates major cell pathways. Cell death & disease 2011;2:e141.
7. Behl C. Breaking BAG: The Co-Chaperone BAG3 in Health and Disease. Trends in pharmacological sciences 2016;37(8):672-688.
8. Liu BQ, Zhang S, Li S et al. BAG3 promotes stem cell-like phenotype in breast cancer by upregulation of CXCR4 via interaction with its transcript. Cell death & disease 2017;8(7):e2933.

9. Qiu S, Sun L, Zhang Y, Han S. Downregulation of BAG3 attenuates cisplatin resistance by inhibiting autophagy in human epithelial ovarian cancer cells. Oncology letters 2019;18(2):1969-1978.
10. Li N, Chen M, Cao Y et al. Bcl-2-associated athanogene 3(BAG3) is associated with tumor cell proliferation, migration, invasion and chemoresistance in colorectal cancer. BMC cancer 2018;18(1):793.
11. Song F, Wang G, Ma Z, Ma Y, Wang Y. Silencing of BAG3 inhibits the epithelial-mesenchymal transition in human cervical cancer. Oncotarget 2017;8(56):95392-95400.
12. Cotugno R, Basile A, Romano E, Gallotta D, Belisario MA. BAG3 down-modulation sensitizes HPV18(+) HeLa cells to PEITC-induced apoptosis and restores p53. Cancer letters 2014;354(2):263-271.
13. Sondermann H, Scheufler C, Schneider C, Hohfeld J, Hartl FU, Moarefi I. Structure of a Bag/Hsc70 complex: convergent functional evolution of Hsp70 nucleotide exchange factors. Science 2001;291(5508):1553-1557.
14. Shi H, Xu H, Li Z et al. BAG3 regulates cell proliferation, migration, and invasion in human colorectal cancer. Tumour biology : the journal of the International Society for Oncodevelopmental Biology and Medicine 2016;37(4):5591-5597.
15. Zhu H, Wu W, Fu Y et al. Overexpressed BAG3 is a potential therapeutic target in chronic lymphocytic leukemia. Annals of hematology 2014;93(3):425-435.
16. Gentilella A, Khalili K. BAG3 expression in glioblastoma cells promotes accumulation of ubiquitinated clients in an Hsp70-dependent manner. The Journal of biological chemistry 2011;286(11):9205-9215.
17. Raffone A, Travaglino A, D'Antonio A et al. BAG3 expression correlates with the grade of dysplasia in squamous intraepithelial lesions of the uterine cervix. Acta obstetricia et gynecologica Scandinavica 2019.
18. Wang Y, Tian Y. miR-206 Inhibits Cell Proliferation, Migration, and Invasion by Targeting BAG3 in Human Cervical Cancer. Oncology research 2018;26(6):923-931.
19. Flum M, Kleemann M, Schneider H et al. miR-217-5p induces apoptosis by directly targeting PRKCI, BAG3, ITGAV and MAPK1 in colorectal cancer cells. Journal of cell communication and signaling 2018;12(2):451-466.
20. Mehta AM, Mooij M, Brankovic I, Ouburg S, Morre SA, Jordanova ES. Cervical Carcinogenesis and Immune Response Gene Polymorphisms: A Review. Journal of immunology research 2017;2017:8913860.
21. Green DR, Galluzzi L, Kroemer G. Cell biology. Metabolic control of cell death. Science 2014;345(6203):1250256.
22. Pavlova NN, Thompson CB. The Emerging Hallmarks of Cancer Metabolism. Cell metabolism 2016;23(1):27-47.
23. Dixon SJ, Lemberg KM, Lamprecht MR et al. Ferroptosis: an iron-dependent form of nonapoptotic cell death. Cell 2012;149(5):1060-1072.

24. Stockwell BR, Friedmann Angeli JP, Bayir H et al. Ferroptosis: A Regulated Cell Death Nexus Linking Metabolism, Redox Biology, and Disease. Cell 2017;171(2):273-285.
25. Bertrand RL. Iron accumulation, glutathione depletion, and lipid peroxidation must occur simultaneously during ferroptosis and are mutually amplifying events. Medical hypotheses 2017;101:69-74.
26. Xie Y, Zhu S, Song X et al. The Tumor Suppressor p53 Limits Ferroptosis by Blocking DPP4 Activity. Cell reports 2017;20(7):1692-1704.
27. Xie Y, Hou W, Song X et al. Ferroptosis: process and function. Cell death and differentiation 2016;23(3):369-379.
28. Zhang Y, Tan H, Daniels JD et al. Imidazole Ketone Erastin Induces Ferroptosis and Slows Tumor Growth in a Mouse Lymphoma Model. Cell chemical biology 2019;26(5):623-633 e629.
29. Yu Y, Xie Y, Cao L et al. The ferroptosis inducer erastin enhances sensitivity of acute myeloid leukemia cells to chemotherapeutic agents. Molecular & cellular oncology 2015;2(4):e1054549.
30. Hao S, Yu J, He W et al. Cysteine Dioxygenase 1 Mediates Erastin-Induced Ferroptosis in Human Gastric Cancer Cells. Neoplasia 2017;19(12):1022-1032.
31. Wang W, Green M, Choi JE et al. CD8(+) T cells regulate tumour ferroptosis during cancer immunotherapy. Nature 2019;569(7755):270-274.
32. Lang X, Green MD, Wang W et al. Radiotherapy and immunotherapy promote tumoral lipid oxidation and ferroptosis via synergistic repression of SLC7A11. Cancer discovery 2019.

Figures

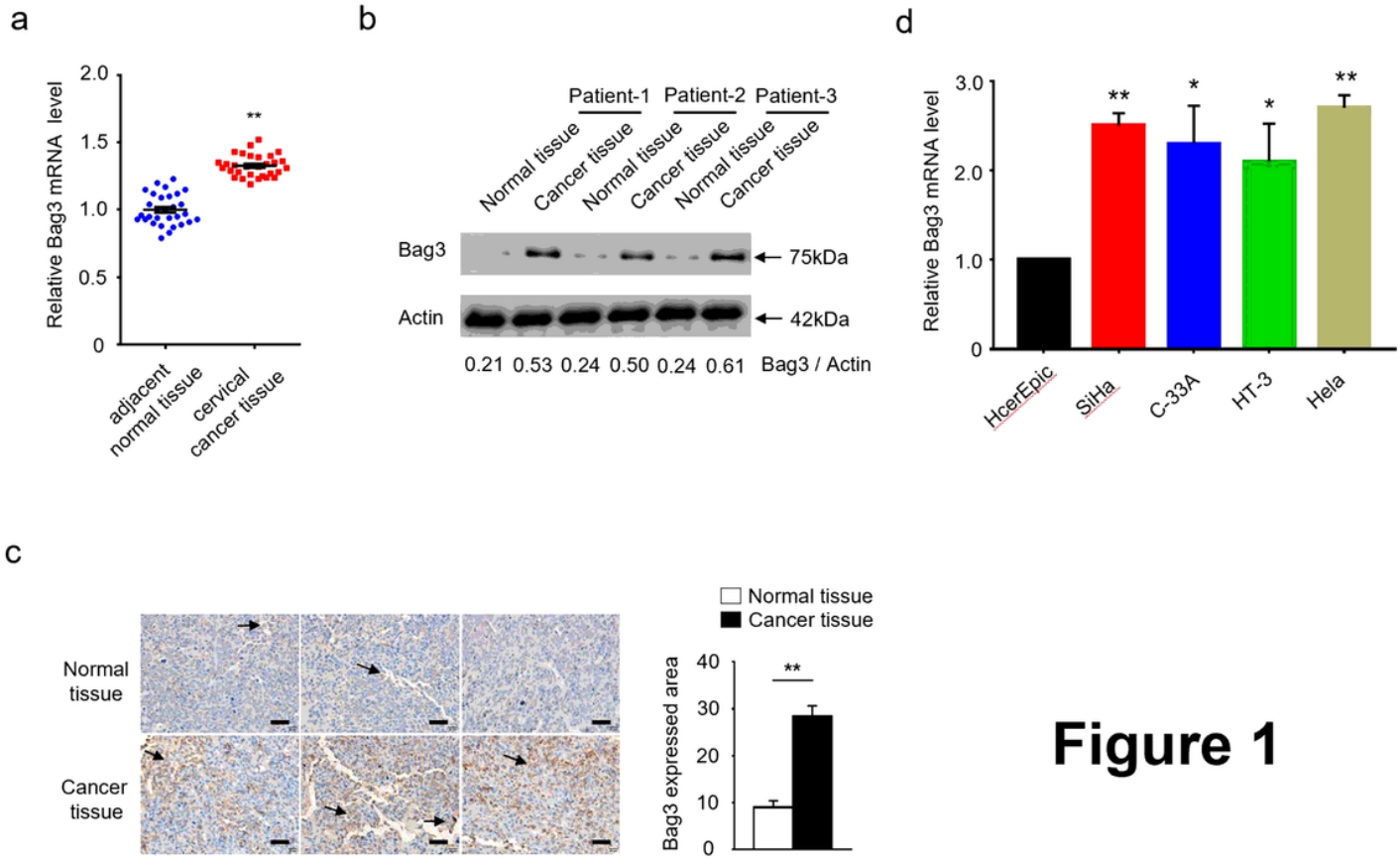

Figure 1

Figure 1

Bag3 is overexpressed in cervical cancer. (a) qRT-PCR analysis of Bag3 levels in adjacent normal tissues and cervical cancer tissues from patients. Data are presented as the mean ± SD (n=30). (b) IB analysis Bag3 protein levels in adjacent normal tissues and cervical cancer tissues from 3 random patients. (c) Immunohistochemistry of Bag3 in adjacent normal tissues and cervical cancer tissues from patients. (d) Bag3 mRNA levels in different cell types were analyzed by qRT-PCR. Data is representative of at least three independent experiments and is presented as the mean ± SD. ns, not statistically significant; * P < 0.05; ** P < 0.01.

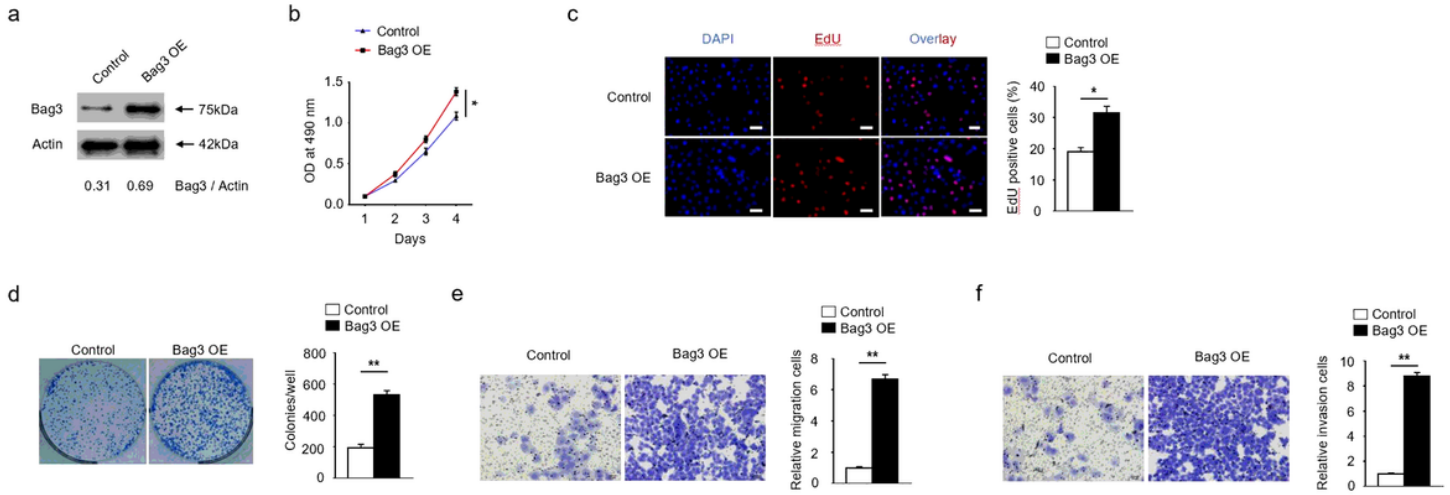

Figure 2

Figure 2

Bag3 promotes the progress of cervical cancer. Bag3 was overexpressed in SiHa cells with lentivirus infection. (a) IB analysis Bag3 levels in SiHa cells. (b) CCK8 assay of SiHa cells. (c) Edu assay analysis of proliferation of SiHa cells. (d) Colony formation assay of SiHa cells. (e) Bar= 20μM. Transwell migration assay of SiHa cells (f) Bar= 20μM. Transwell invasion assay of SiHa cells Data are representative of at least three independent experiments and are presented as the mean ± SD. ns, not statistically significant; * P < 0.05; ** P < 0.01.

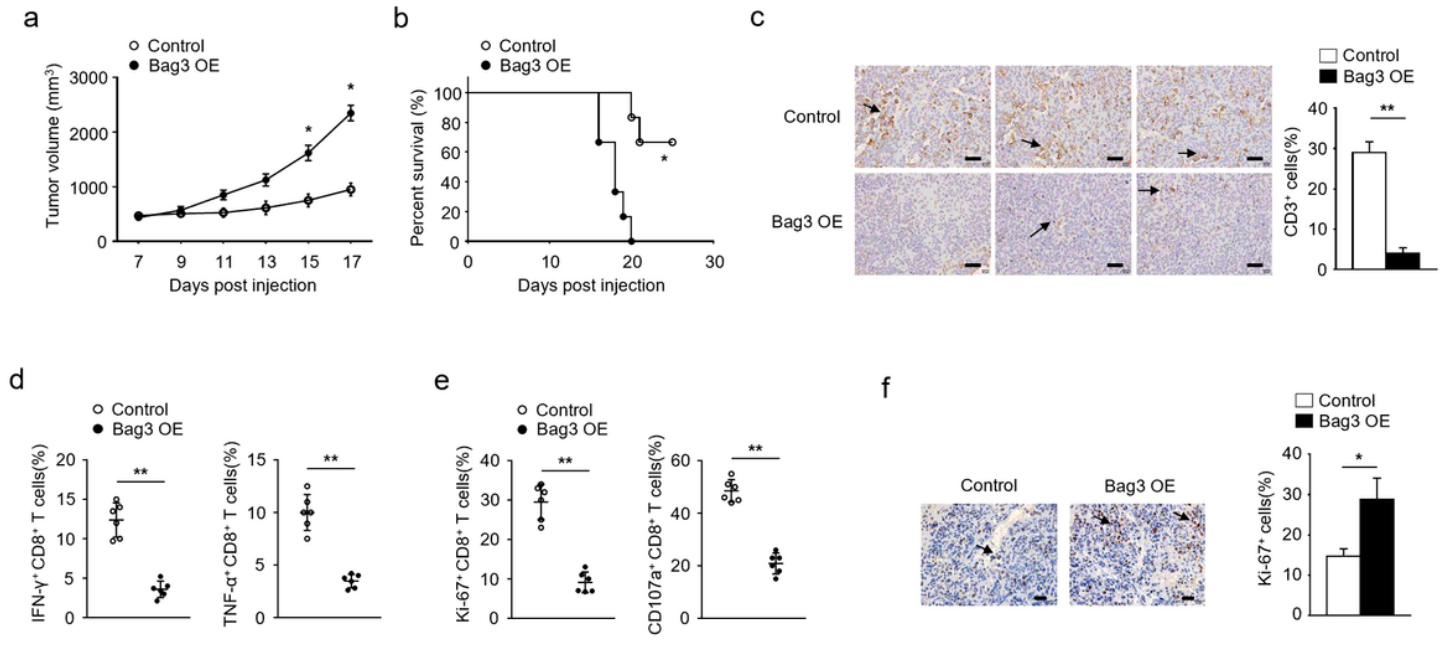

Figure 3

Figure 3

Bag3 impairs the immune response in cervical cancer. (a-b) Tumor growth curve and survival curve of mice that received control and Bag3-overexpressed SiHa cells injected orthotopically. (c) Immunohistochemical staining for CD3 and quantification of infiltrating CD3+ T cells around tumors. Arrows indicate CD3. (d) Quantification of the frequency of IFN-γ- or TNF-α-producing CD8+ T cells in tumor sections by flow cytometry. (e) Quantification of the frequency of Ki-67+- or CD107a-producing CD8+ T cells in tumor sections by flow cytometry. (f) Immunohistochemical analysis of Ki-67 levels in tumors. Arrows indicate Ki-67. Data is representative of at least three independent experiments and is presented as the mean ± SD. ns, not statistically significant; * $P < 0.05$; ** $P < 0.01$.

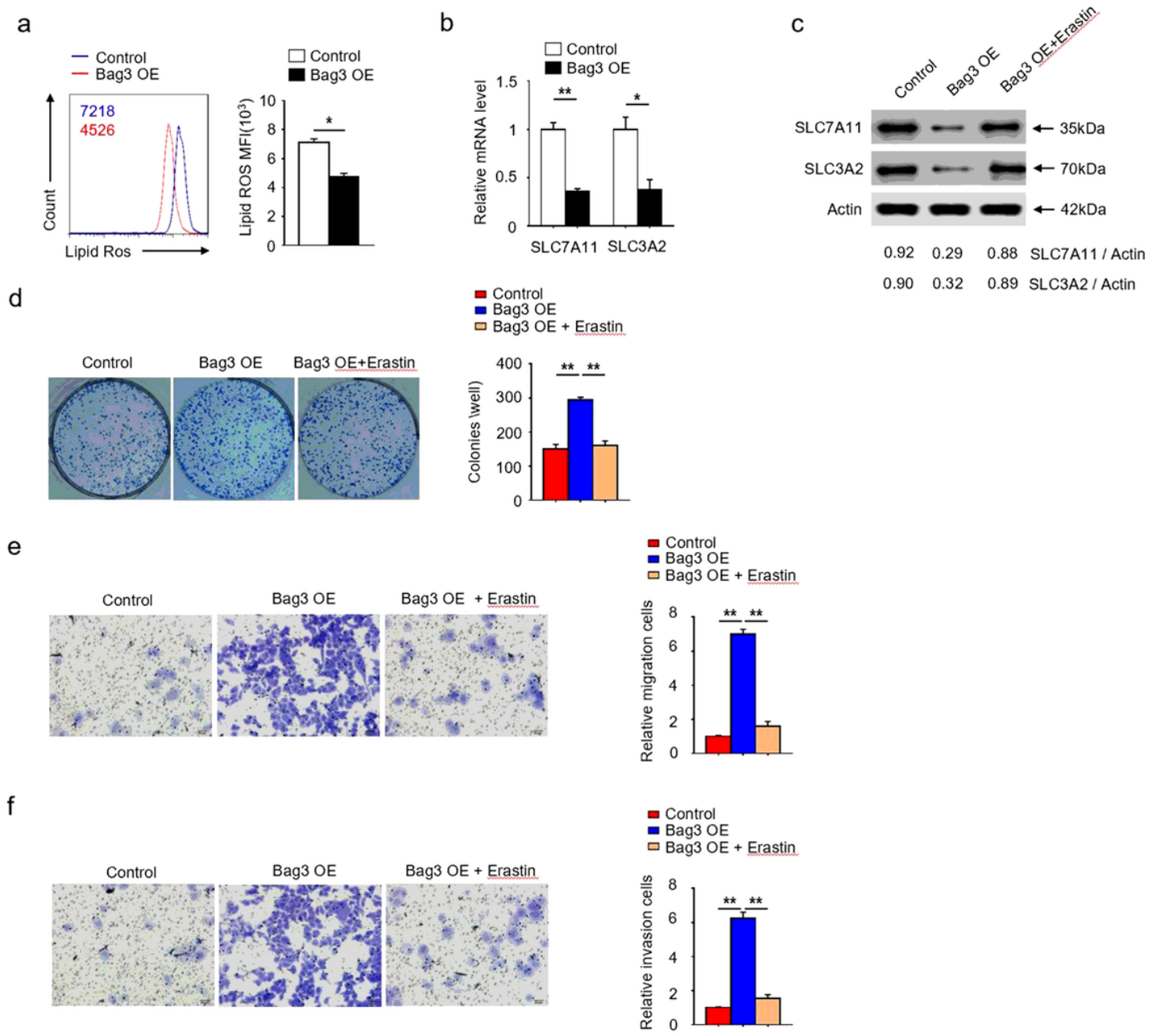

Figure 4

Figure 4

Bag3 inhibits ferroptosis of SiHa cells. (a) Flow cytometry analysis of BODIPY fluorescence of control and Bag3 OE SiHa cells. (b) SLC7A11 and SLC3A2 mRNA levels in control and Bag3 OE SiHa cells were analyzed by qRT-PCR. (c) IB analysis of SLC7A11 and SLC3A2 protein levels in SiHa cells in the presence of ferroptosis inducer-Erastin (1μM). (d) Colony formation assay of SiHa cells in the presence of Erastin (1μM). (e) Bar= 20μM. Transwell migration assay of SiHa cells in the presence of Erastin (1μM). (f) Bar= 20μM. Transwell invasion assay of SiHa cells in the presence of Erastin (1μM). Data is representative of

at least three independent experiments and is presented as the mean ± SD. ns, not statistically significant; * P < 0.05; ** P < 0.01.

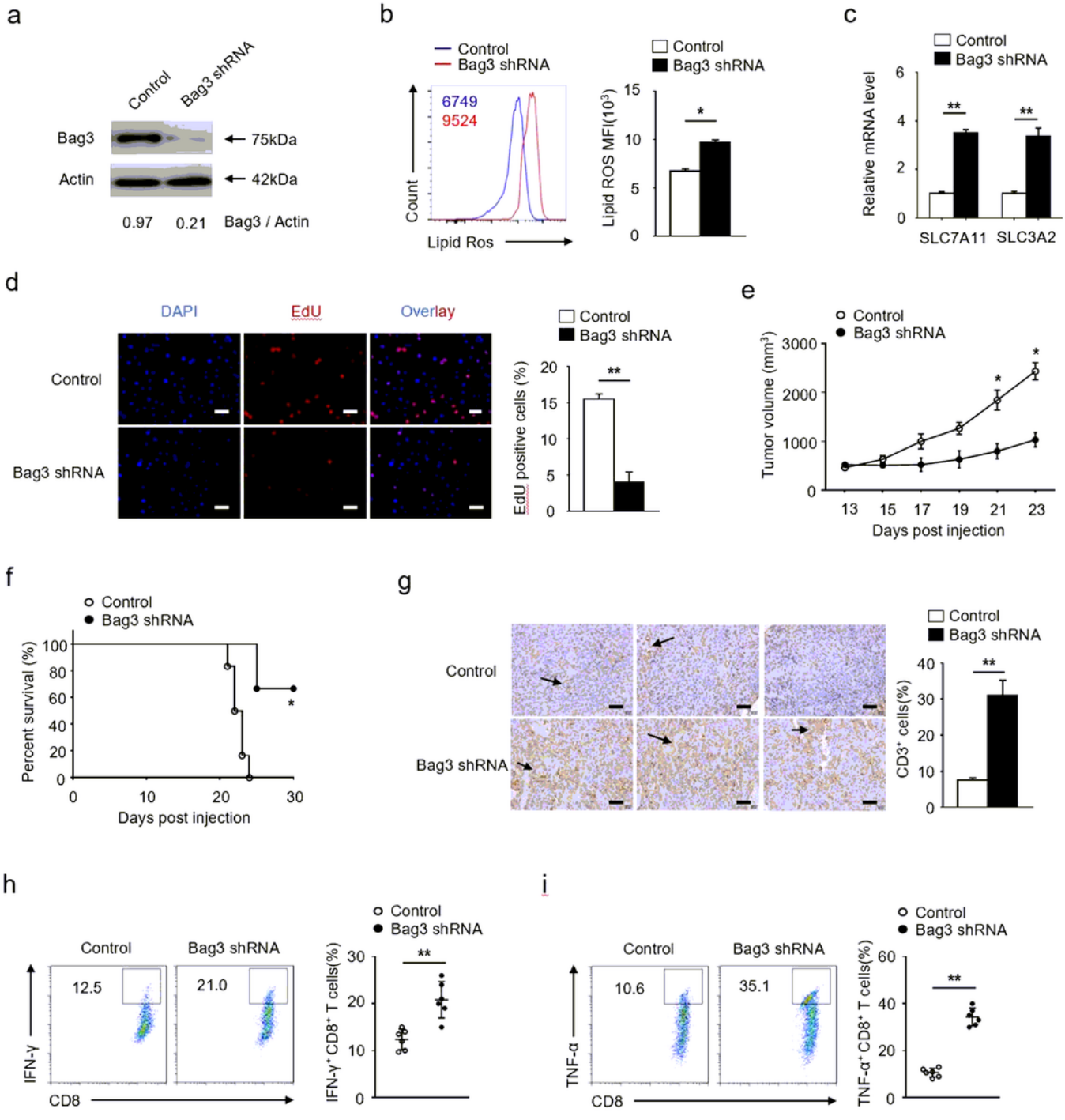

Figure 5

Figure 5

Bag3 deletion ameliorates the development of cervical cancer (a) IB analysis Bag3 protein levels in SiHa cells infected with Bag3 shRNA. (b) Flow cytometry analysis of BODIPY fluorescence of control and Bag3 shRNA SiHa cells. (c) SLC7A11 and SLC3A2 mRNA levels in control and Bag3 shRNA SiHa cells were

analyzed by qRT-PCR. (d) EdU assay analysis of proliferation of Bag3 shRNA SiHa cells. For (e-i) control and Bag3-shRNA SiHa cells were injected orthotopically into mice. (e and f) Tumor growth curve and survival curve of mice that received control and Bag3-overexpressed SiHa cell injection. (g) Immunohistochemical staining of CD3 and quantification of infiltrating CD3+ T cells around tumors. Arrows indicate CD3. (h and i) Quantification of the frequency of IFN-γ- or TNF-α-producing CD8+ T cells in tumor sections by flow cytometry. Data are representative of at least three independent experiments and are presented as the mean ± SD. ns, not statistically significant; * $P < 0.05$; ** $P < 0.01$.